Available online at www.sciencedirect.com
SCIENCE DIRECT
ELSEVIER
Materials Science in Semiconductor Processing 6 (2003) 503–506
MATERIALS SCIENCE IN SEMICONDUCTOR PROCESSING

High-energy photoemission spectroscopy of ferromagnetic $Ga_{1-x}Mn_xN$

J.J. Kim[a,*], H. Makino[a], P.P. Chen[a], T. Hanada[a], T. Yao[a], K. Kobayashi[b], M. Yabashi[b], Y. Takata[c], T. Tokushima[c], D. Miwa[c], K. Tamasaku[c], T. Ishikawa[c], S. Shin[c], T. Yamamoto[d]

[a] *Institute for Materials Research, Tohoku University, Sendai 980-8577, Japan*
[b] *JASRI/SPring-8, 1-1-1 Kouto, Mikazuki-cho, Sayo-gun, Hyogo 679-5198, Japan*
[c] *RIKEN/SPring-8, 1-1-1 Kouto, Mikazuki-cho, Sayo-gun, Hyogo 679-5148, Japan*
[d] *Department of Electronic and Photonic Systems Engineering, Kochi University of Technology, 185 Miyanokuchi, Tosayamada-cho, Kamigun, Kochi 782-8502, Japan*

Abstract

Here we report investigation of valence band electronic states of ferromagnetic $Ga_{0.96}Mn_{0.04}N$ by bulk-sensitive X-ray photoemission, which is realized at high flux X-ray undulator beamline BL29XU of SPring-8, at photon energy of 5.95 keV. We have observed that Mn doping introduces a new structure in the band gap region near the top of the valence band, and also a broader structure in deeper valence band region. Basing upon the first principle calculation, these structures are assigned as Ga 4s originated states, which are raised by hybridization between 3d orbitals of Mn with GaN host orbitals. The present result evidences the second nearest Ga bonds are affected by that Mn–N bond formation, suggesting the long-range interaction of Mn in this host material.
© 2003 Elsevier Ltd. All rights reserved.

PACS: 75.30.Hx; 79.60.Bm

Keywords: High-energy photoemission spectroscopy; GaMnN; Ferromagnetism

1. Introduction

In the spintronics, two degrees of freedom, namely, charge of electron and spin of it, have been explored to look into the possibility of realizing new functionalities. The discovery of the carrier-induced ferromagnetism in InMnAs and GaMnAs have been of much interest in this point of view [1]. However, the highest Curie temperature (T_c) reported is 110 K for GaMnAs, being far from room temperature. Recently, Dietl et al. have calculated T_c using the Zener model for 5% Mn in various II/VI and III/V compound semiconductors and predicted that GaMnN has a T_c above room temperature [2, 3] and Sato et al. have suggested that the V-, Cr-, Mn-doped GaN are promising candidates as room temperature ferromagnetic diluted magnetic semiconductor (DMS) by first principle calculation [4]. These predictions led to recent flurry of investigations on ferromagnetism in GaMnN. Various T_c which scatters in the wide range from 10 to 940 K [5–9] has been reported by measurements of magnetic property in this material. Meanwhile, it is argued that the observed ferromagnetism arose from ferromagnetic GaMn clusters [10]. Recent progress in the first principle calculations of valence band structure enables us to predict the magnetism in the DMSs. Thus the valence band structure is the most basic and necessary information to understand the magnetic and transport properties basing upon these calculations to solve the controversial

*Corresponding author. Fax: +81-22-215-2073.
E-mail address: jungjin@imr.tohoku.ac.jp (J.J. Kim).

1369-8001/$ - see front matter © 2003 Elsevier Ltd. All rights reserved.
doi:10.1016/j.mssp.2003.07.023

situation mentioned above. Photoemission spectroscopy is one of the most powerful tools to investigate the electronic structure of a material. In this work, we report on the result of bulk sensitive high-resolution XPS at 5.95 keV photon energy performed at X-ray undulator beamline BL29XU [11,12] of SPring-8. The valence band spectra obtained in $Ga_{0.96}Mn_{0.04}N$ and GaN are real bulk sensitive, and also almost free from distortion due to inelastic scattering in this high-energy region [13,14]. Thus we are able to give precise analysis of the difference spectra between the doped and non-doped GaN based upon the theoretical calculation results.

2. Experiment

GaN and $Ga_{0.96}Mn_{0.04}N$ films were grown by N_2 plasma-assisted MBE on *c*-axis oriented Al_2O_3 substrate. Details about growth process, structural, and magnetic properties will be published, elsewhere [15].

The photoemission spectra of $Ga_{0.96}Mn_{0.04}N$ and GaN grown by MBE have been measured using synchrotron radiation from SPring-8. High-energy X-ray of 5.95 keV with an energy spread of 75 meV was used. The very large escape depth at high energy (above 5 nm at 5.95 keV) would allow determination of bulk electronic states with high preciseness owing to very small contribution from surface. Therefore, no surface cleaning was done. Photoelectrons were collected using the SCIENTA hemispherical analyzer. The energy resolution was estimated to be 240 meV from the Fermi edge of gold (Au) plates.

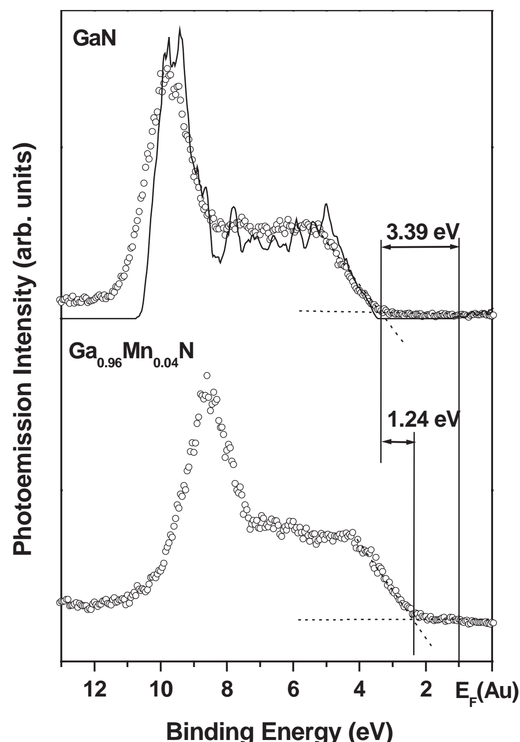

Fig. 1. Normalized valence EDC for the GaN and $Ga_{0.96}Mn_{0.04}N$. The solid curve, in the EDC of GaN, is fitted value by linear combination of pDOS [14]. There was the binding energy difference between them about 1.24 eV caused by band bending to the surface.

3. Results and discussion

Fig. 1 shows the valence band spectra for the GaN and $Ga_{0.96}Mn_{0.04}N$. Intensity of the spectra has been normalized to Ga 3d core level peaks. Because GaN is intrinsic n-type semiconductor, the energy difference between Fermi energy (E_F) and valence band maximum (VBM) is nearly the same with band gap energy. Fig. 1 shows the difference between the top of valence energy distribution curve (EDC) and the E_F of Au is 3.39 eV and this corresponds to band gap energy of GaN ($E_g = 3.39$ eV). However, in case of $Ga_{0.96}Mn_{0.04}N$, the top of valence EDC is shifted to 1.24 eV lower binding energy. This shift is attributed to the E_F pinning by Mn transition metal impurity state in band gap. In $Ga_{0.96}Mn_{0.04}N$, the energy difference between the top of valence EDC and the E_F of Au is 2.15 eV and this value coincides with the energy difference between the VBM and E_F of $Ga_{0.94}Mn_{0.06}N$ density of states (DOS), which are calculated by first principle calculation (Fig. 3(b)). Measured valence EDC of GaN is well fitted by a linear combination of partial DOS [14], as shown by solid curve in Fig. 1. Main contribution of the resultant calculated EDC comes from the Ga 4s partial DOS. This can be explained in terms of the atomic subshell photoionization cross sections as functions of the photon energy [16]. We depicted photon energy dependence of Ga 4s, N 2p, N 2s, and Mn 3d subshell cross sections in Fig. 2, to show that the Mn 3d and N 2p contributions are negligible at 5.95 keV.

To compare the electronic structure difference between $Ga_{0.96}Mn_{0.04}N$ and GaN, GaN valence EDC was shifted to the low binding energy 1.24 eV. Fig. 3(a) shows the valence EDC of $Ga_{0.96}Mn_{0.04}N$, GaN and the difference spectra between them. One can clearly see the difference between the valence EDC of GaN and that of $Ga_{0.96}Mn_{0.04}N$ from 5.5 to 7.5 eV and about 1.5 eV.

In order to elucidate the different electronic structure between $Ga_{0.96}Mn_{0.04}N$ and pure GaN, we have obtained the theoretical DOS by first principle calculation, which suggests that $Ga_{0.94}Mn_{0.06}N$ is ferromagnetic. The details of calculation will be discussed, elsewhere. Fig. 3(b) shows these calculated total DOS of $Ga_{0.94}Mn_{0.06}N$ and Mn 3d partial DOS of it. The t^b

state means the bonding state comes from the hybridization between Mn 3dε orbitals which are consisting of d_{xy}, d_{yz}, and d_{zx} orbitals and 2p orbitals of four N atoms close to the Mn atom and the t^a state means anti-bonding state corresponds to the bonding state. The e state means non-bonding state caused by Mn 3dγ orbitals which are consisting of $d_{x^2-y^2}$ and d_{z^2} orbitals. In the tetrahedral symmetry, dε orbitals with T_2 symmetry can be only hybridized with the ligand orbitals. Therefore, Mn dε orbitals can make bonding state and anti-bonding state by hybridization with the 2p orbitals of four N atoms close to the Mn. Because the symmetry, E, of Mn dγ orbitals do not coincide with the symmetry, A_1 and T_2, of the ligand group orbitals, Mn dγ orbitals weakly interact with the N atoms described above, making a non-bonding energy state.

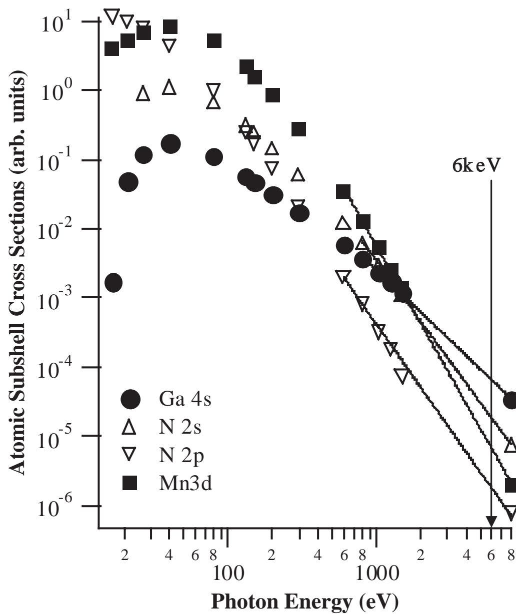

Fig. 2. Atomic subshell photoionization cross sections according to photon energy calculated by Yeh and Lindau [16]. The data between 1486.6 and 8047.8 eV was interpolated using $y = Ax^b$ equation.

Now we discuss the origin of the difference between the electronic structure of $Ga_{0.96}Mn_{0.04}N$, which showed ferromagnetism up to 200 K [15], and pure GaN by comparison with theoretically calculated DOS. In difference spectrum (Fig. 3(a)) between $Ga_{0.96}Mn_{0.04}N$ and GaN valence EDC, the broad state range from 5.5 to 7.5 eV is similar to t^b state of calculated DOS (Fig. 3(b)) and the state about 1.5 eV is similar to e state of calculated one. Because the measured valence EDC is dominated by Ga 4s contribution as mentioned above at this high photon energy, structures in the difference spectrum cannot be attributed to Mn 3d states. Simple and direct interpretation of the present result is that second nearest neighbor Ga bonding with nearest N is also affected by the Mn–N bond formation.

Okabayashi et al. [17] reported the different electronic structure between $In_{1-x}Mn_xAs$ ($T_c \leqslant 55$ K) and $Ga_{1-x}Mn_xAs$ ($T_c \leqslant 110$ K) at valence band maximum by angle-resolved photoemission spectroscopy in the 46–55 eV photon energy region where Mn 3d

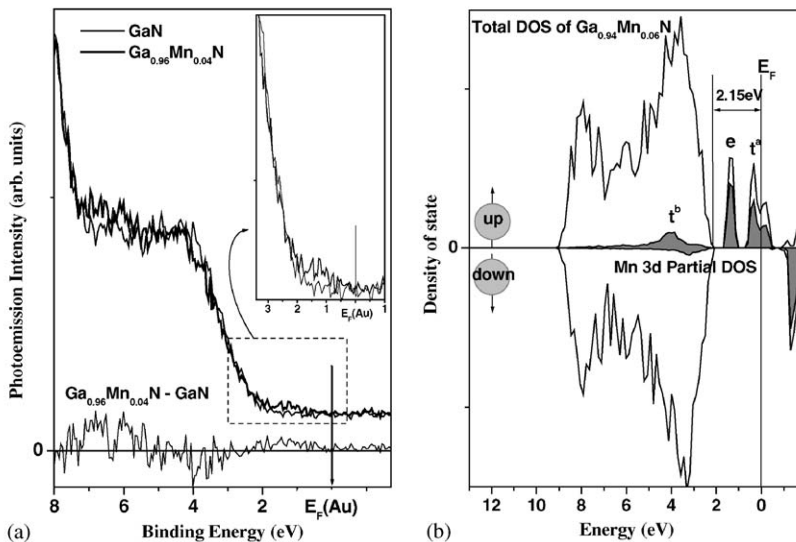

Fig. 3. (a) Valence EDC of shifted GaN to the lower binding energy about 1.24 eV and $Ga_{0.96}Mn_{0.04}N$ and the difference spectra between them. (b) Total DOS of $Ga_{0.94}Mn_{0.06}N$ (Solid line) and Mn 3d pDOS (Gray region) calculated by first principle band calculation. t^b means bonding state, t^a means anti-bonding state, e means non-bonding state, E_F means Fermi energy.

photoionization cross section dominates but surface sensitivity is very high. In case of $Ga_{1-x}Mn_xAs$, there were new states near the valence band maximum by Mn doping. Although Mn doping in GaAs induced split-off states above the VBM through hybridization with As 4p and forms the impurity-band like states, Mn in InAs did not induce such states, probably because of the weaker hybridization strength caused by longer Mn–As bond length in $In_{1-x}Mn_xAs$ (0.254–0.258 nm [18]) than that in GaAs (0.244 nm [19]), and smaller band gap of InAs compared to those of GaAs.

In case of $Ga_{1-x}Mn_xN$, Mn–N distance was estimated to be $\leqslant 0.2$ nm [20] by EXAFS analysis. This means that Mn–N hybridization is to be much stronger than that in $Ga_{1-x}Mn_xAs$. The hybridization gives rise to Mn induced states as already discussed in the text. The larger GaN band gap (3.39 eV) tends to localize the Mn induced states. Thus main part of the states appears in the band gap region. Stronger hybridization also causes indirect hybridization of Ga 4s and Ga 4p through Ga–N bond. Our first principle local density of state calculation showed that spin polarized band gap states appears in the nearest N and second nearest Ga bonds. The present results evidence the long-range effect of the Mn on the chemical bonding of matrix, which is expected to be a key to understand high T_c in $Ga_{1-x}Mn_xN$. It should be noticed that we measured the spectra of the samples without surface cleaning procedure because of high bulk sensitivity of the high-energy XPS. Therefore, the present spectra are free from spurious effects such as surface segregation and surface defects, which might be introduced during surface cleaning procedure.

4. Conclusion

We have investigated the electronic structure of $Ga_{0.96}Mn_{0.04}N$ using high-energy bulk sensitive hard X-ray photoemission spectroscopy using synchrotron radiation. We have observed the new electronic states just above valence band maximum and in valence band by Mn doping in GaN host. This is attributed to Ga 4s originated state raised by the hybridization between Mn 3d and the valence electrons of GaN host, which may play a significant role in the observed ferromagnetism in $Ga_{0.96}Mn_{0.04}N$.

Acknowledgements

We thank Dr. N. Kamakura for his help in the photoemission spectra measurement in this work.

References

[1] Ohno Y, Young DK, Beschoten B, Matsukura F, Ohno H, Awschalom DD. Nature 1999;402:709.
[2] Dietl T, Ohno H, Matsukura F, Cibert J, Ferrand D. Science 2000;287:1019.
[3] Dietl T, Ohno H, Matsukura F. Phys Rev B 2001;63: 195205.
[4] Sato K, Katayama-Yoshida H. Jpn J Appl Phys 2001;40: L485.
[5] Overberg ME, Abernathy CR, Pearton SJ, Theodoropoulou NA. Appl Phys Lett 2001;79:1312.
[6] Thaler GT, Overberg ME, Gila B, Frazier R, Abernathy CR, Pearton SJ. Appl Phys Lett 2002;80:3964.
[7] Theodoropoulou N, Hebard AF, Overg ME,釐bernthy CR, Pearton SJ. Appl Phys Lett 2001;78:3475.
[8] Reed ML, El-Masry NA, Stadelmaier HH, Ritums MK, Reed MJ. Appl Phys Lett 2001;79:3473.
[9] Sonoda S, Shimizu S, Sasaki T, Yamamoto Y, Hori H. J Cryst Growth 2002;237–239:1358.
[10] Shon Y, Kwon YH, Kim DY, Fan X, Fu D, Kang TW. Jpn J Appl Phys 2001;40:5304.
[11] Kitamura H. Recent trends of insertion-device technology for X-ray sources. J Synchrotron Radiat 2000;7:121–30.
[12] Tamasaku K, Tanaka Y, Yabashi M, Yamazaki H, Kawamura N, Suzuki M, Ishikawa T, SPring-8 RIKEN beamline III for coherent X-ray optics. Nucl Instrum Methods A 2001;467/468: 686–9.
[13] Takata Y, Kobayashi K, Tamasaku K, Miwa D, Ishikawa T, Shin S. Private communication.
[14] Kobayashi K, Takata Y, Yamamoto T, Kim JJ, Makino H, Tamasaku K, Yabashi M, Miwa D, Ishikawa T, Shin S, Yao T. Private communication.
[15] Chen PP, Makino H, Kim JJ, Yao T. J Cryst Growth 2003;251:331.
[16] Yeh JJ, Lindau I. At Data Nucl Data Tables 1985;32:1.
[17] Okabayashi J, Mizokawa T, Sarma DD, Fujimori A, Slupinski T, Oiwa A, Munekata H. Phys Rev B 2002;65: 161203.
[18] Soo YL, Huang SW, Ming ZH, Kao TH, Munekata H, Chang LL. Phys Rev B 1996;53:4905.
[19] Shioda R, Ando K, Hatashi T, Tanaka M. Phys Rev B 1998;58:1100.
[20] Soo YL, Kioseoglou G, Kim S, Huang S, Kao YH, Kuwabara S, Owa S, Kondo T, Munekata YH. Appl Phys Lett 2001;79:3926.